

Supplementary Materials for  
**Condensed but liquid-like domain organization of active chromatin regions in living human cells**

Tadasu Nozaki *et al.*

Corresponding author: Kazuhiro Maeshima, kmaeshim@nig.ac.jp

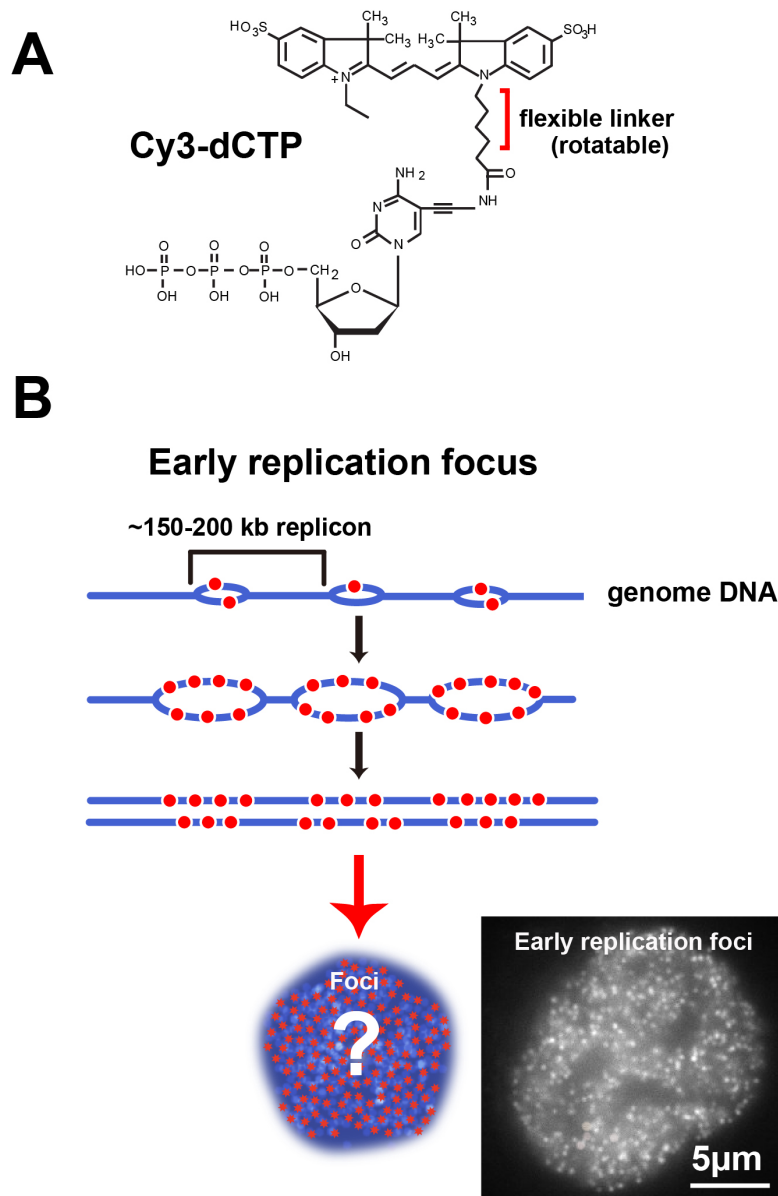
*Sci. Adv.* **9**, eadf1488 (2023)  
DOI: 10.1126/sciadv.adf1488

**The PDF file includes:**

Figs. S1 to S9  
Table S1  
Legends for movies S1 to S16

**Other Supplementary Material for this manuscript includes the following:**

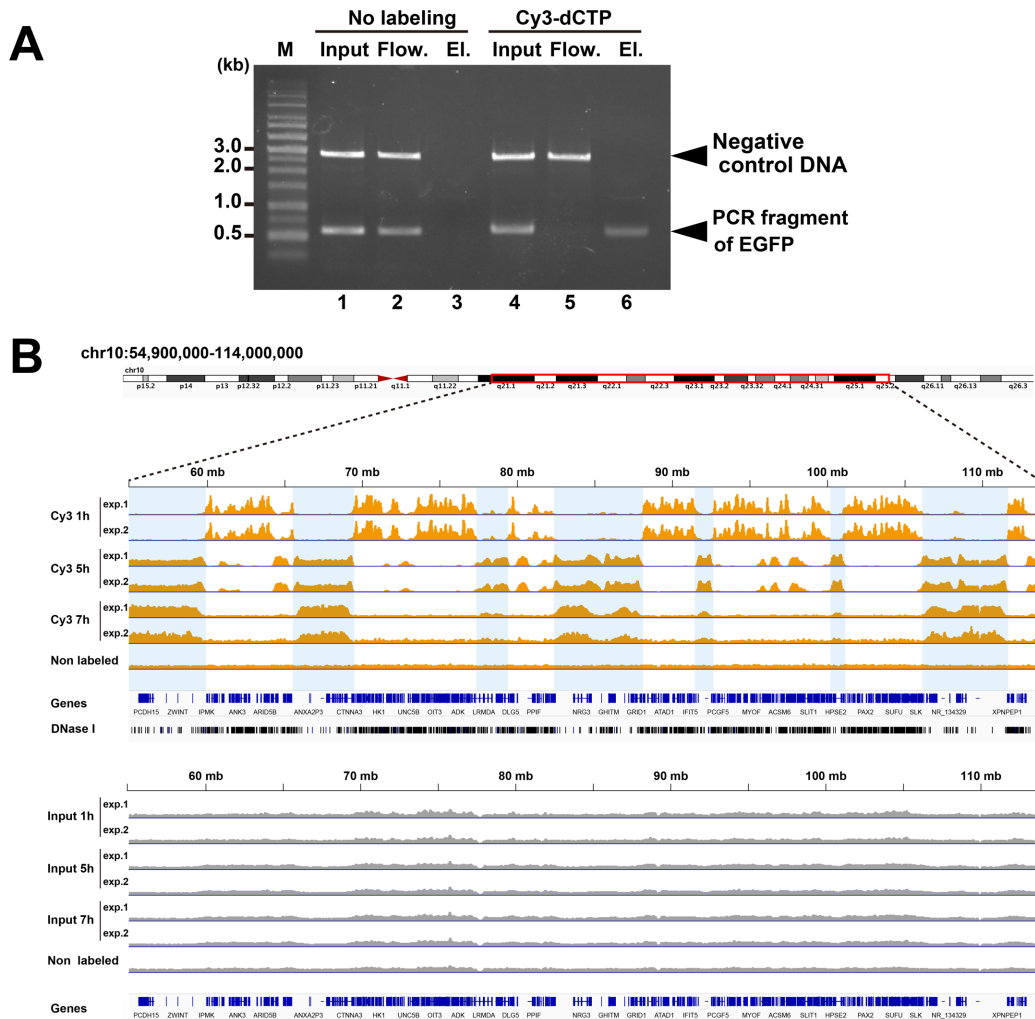
Movies S1 to 16



## Supplemental Figure S1

**Fig. S1. Cy3-dCTP labeling of the early replication foci.**

(A) Structure of Cy3-dCTP. The Cy3 dye is conjugated to a cytosine base. (B) Scheme for Cy3-dCTP (red) incorporation during early DNA replication. Each replication focus was assumed to be a genomic region with one or a few replication units (replicons) (22).

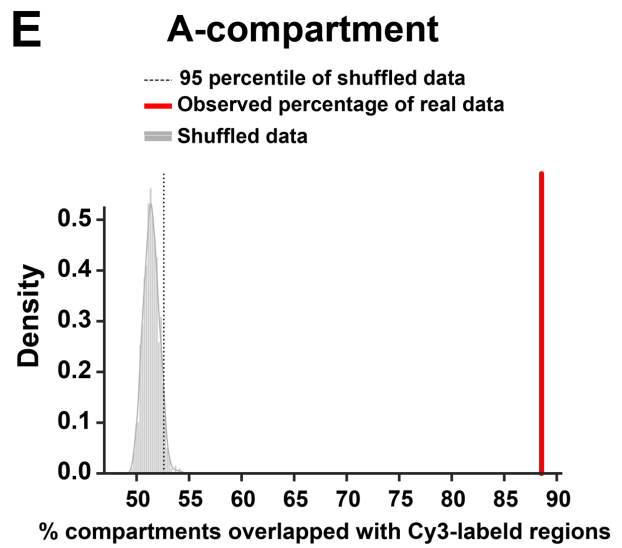
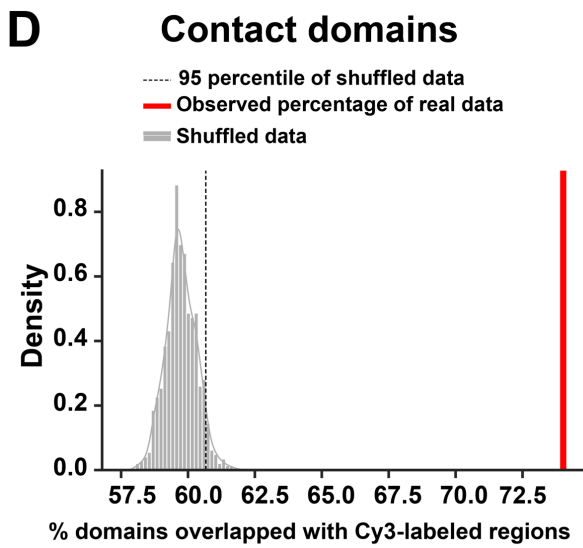
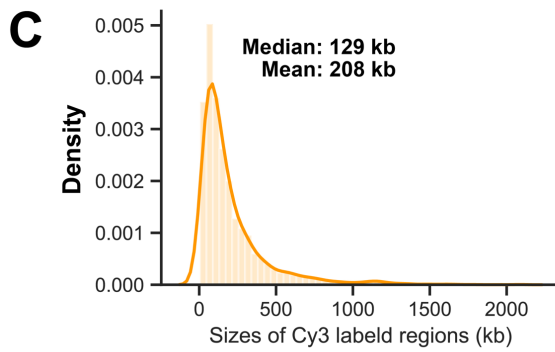


## Supplemental Figure S2

**Fig. S2. Immunoprecipitation of Cy3-labeled DNA regions and the genome sequence analysis by next-generation sequencing.**

(A) Purification of the Cy3-dCTP-containing PCR fragments with anti-Cy3 antibody. Each fraction [input, flow-through (Flow.), eluate (El.)] was analyzed by agarose gel electrophoresis with ethidium bromide staining. The positions of EGFP gene PCR fragments and the negative control DNA (pGEM®-T Easy plasmid after digestion with *EcoRI*) are indicated. A non-labeled PCR fragment was used for the assay (lanes 1–3), and the PCR fragment labeled with Cy3-dCTP was used for the other assay (lane 4–6). M, 1 kb DNA ladder. (B) Visualization of Cy3-labeled DNA regions on chromosome 10\_54,900,000–114,000,000 by the Integrative Genomics Viewer (IGV) Browser. The distributions of the mapped reads of Cy3-dCTP IP samples (upper panel) and input samples (lower panel) from

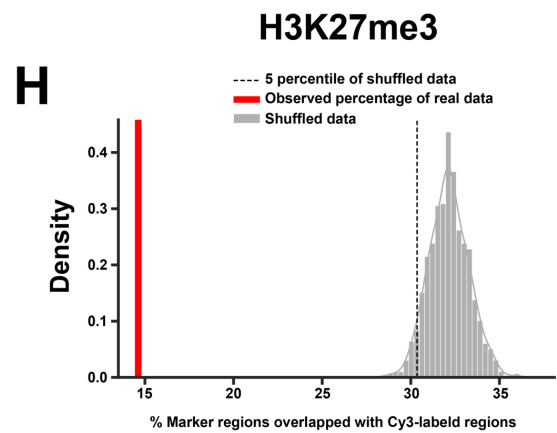
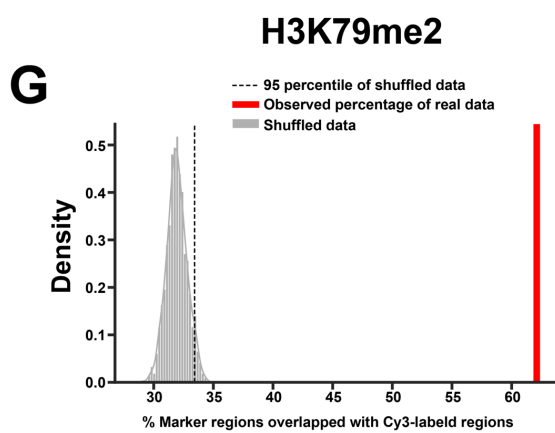
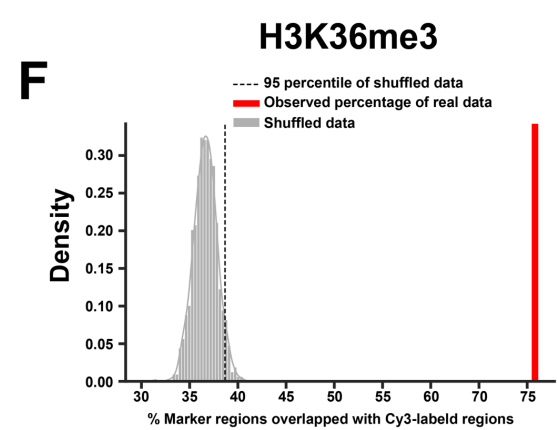
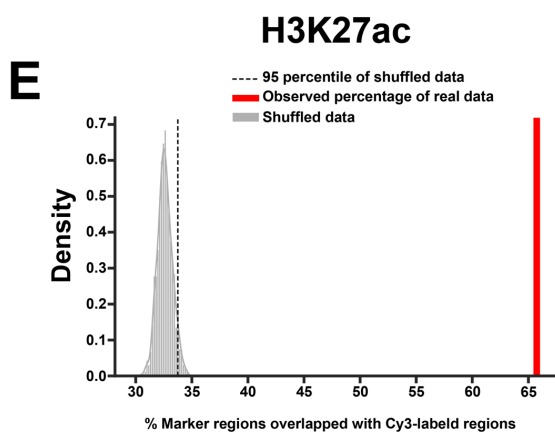
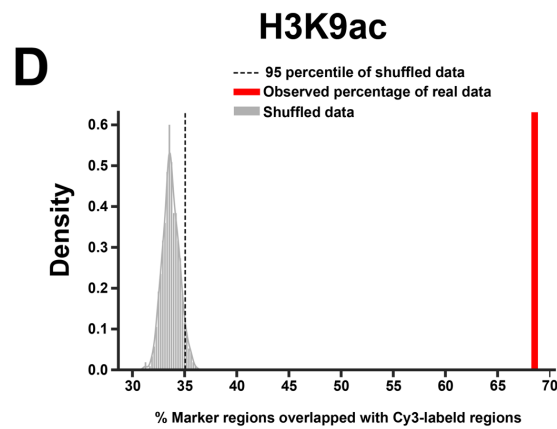
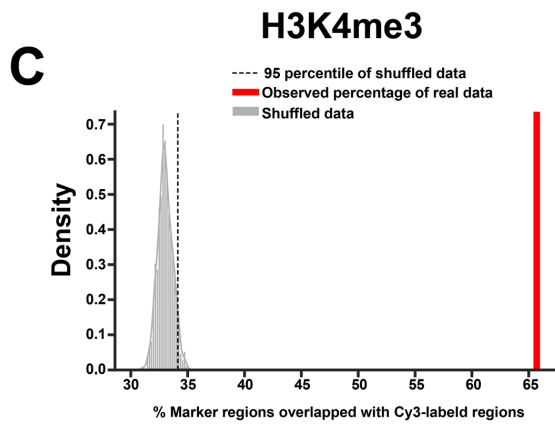
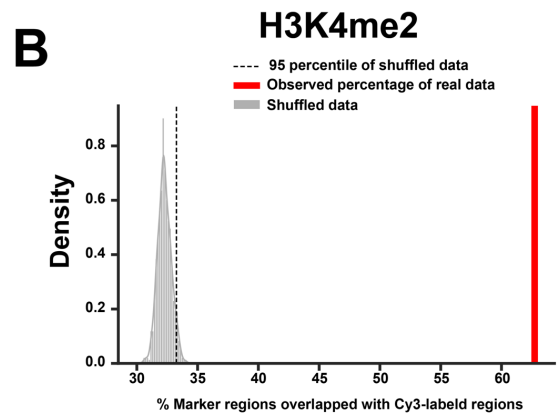
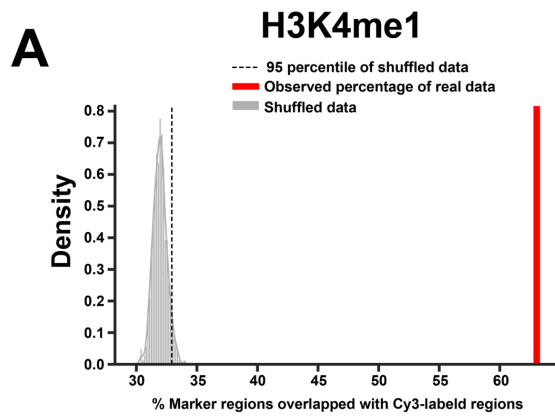
two independent Cy3-labeled DNA pulldown experiments are shown. A non-labeled IP sample was used to detect DNAs that non-specifically bound the beads (lower panel). Cy3-labeled DNA regions at early (1 hour), mid (5 hours), and late (7 hours) S phase were performed from two independent Cy3-labeled DNA pulldown experiments.



**Supplemental Figure S3**

**Fig. S3. Comparisons of Cy3-labeled DNA regions with histone marks and contact domains.**

(A-B) Visualization of Cy3-labeled DNA regions (orange bars), Hi-C contact domains (blue bars), active histone marks (green), and an inactive histone mark (pink) at genomic regions of chr8:25,315,538-27,123,952 (A) and chr7:22,079,950-22,790,390 (B) by the Integrative Genomics Viewer (IGV) Browser. (C) Size (in kb) distribution of Cy3-labeled regions. (D-E) Percentage distribution of regions overlapped with Hi-C contact domains (D) and A-compartment (E) in each of the 1,000 randomly shuffled datasets. The dotted line shows the 95th percentile of the shuffled distribution and the red solid line shows the percentage observed in the real dataset of Cy3-labeled regions.

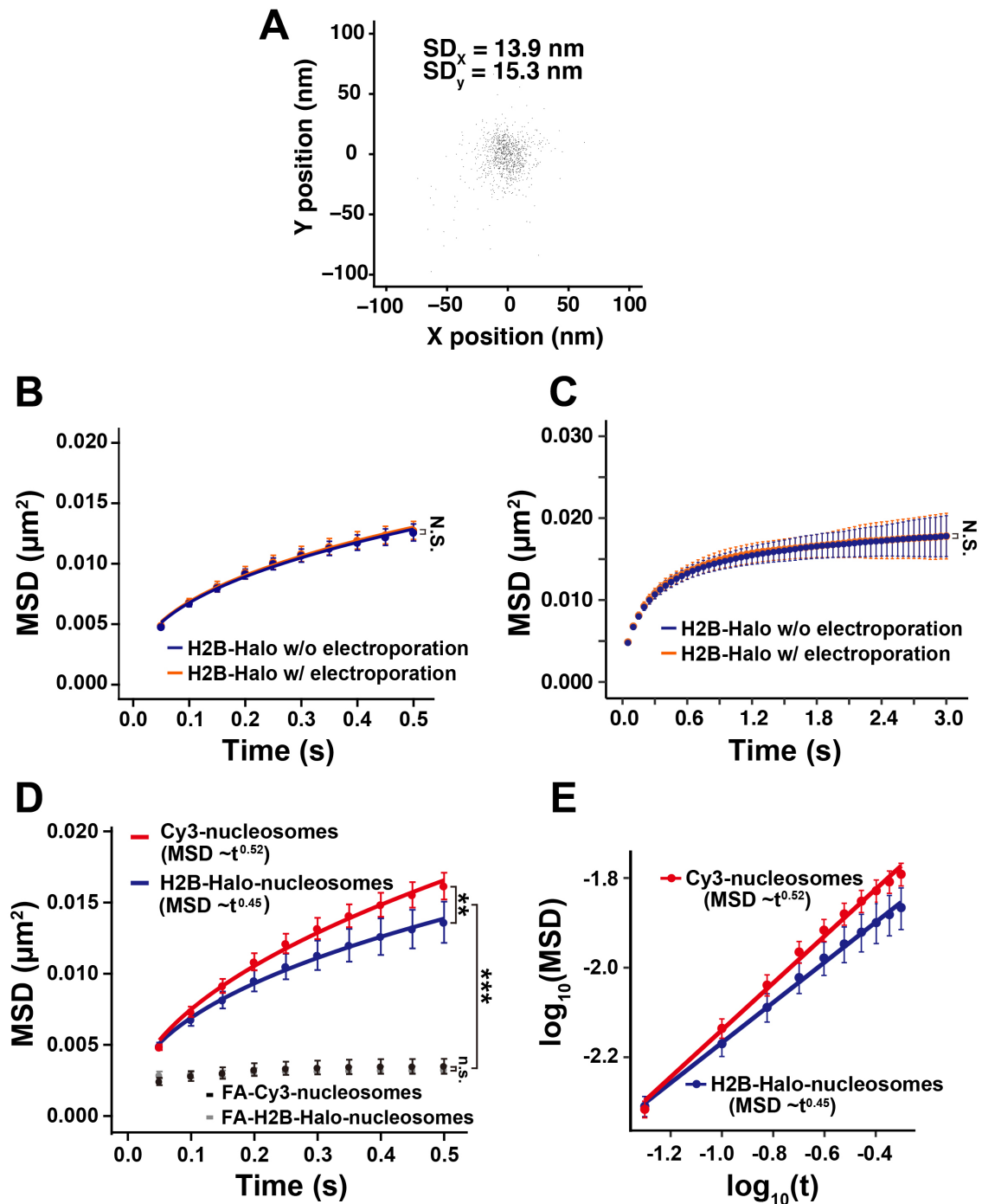


**Supplemental Figure S4**

**Fig. S4. Statistical analysis between histone marks and Cy3-labeled regions.**

Distributions of percentages of active histone marks (A) H3K4me1, (B) H3K4me2, (C) H3K4me3, (D) H3K9ac, (E) H3K27ac, (F) H3K36me3, (G) H3K79me2, and an inactive histone mark (H) H3K27me3 were overlapped with 1,000 randomly shuffled datasets of Cy3-labeled regions. The red solid line shows the percentage observed in the real dataset of Cy3-labeled regions and the dotted line shows the 95th percentile (A-G), or the 5th percentile (H), of the shuffled distribution.



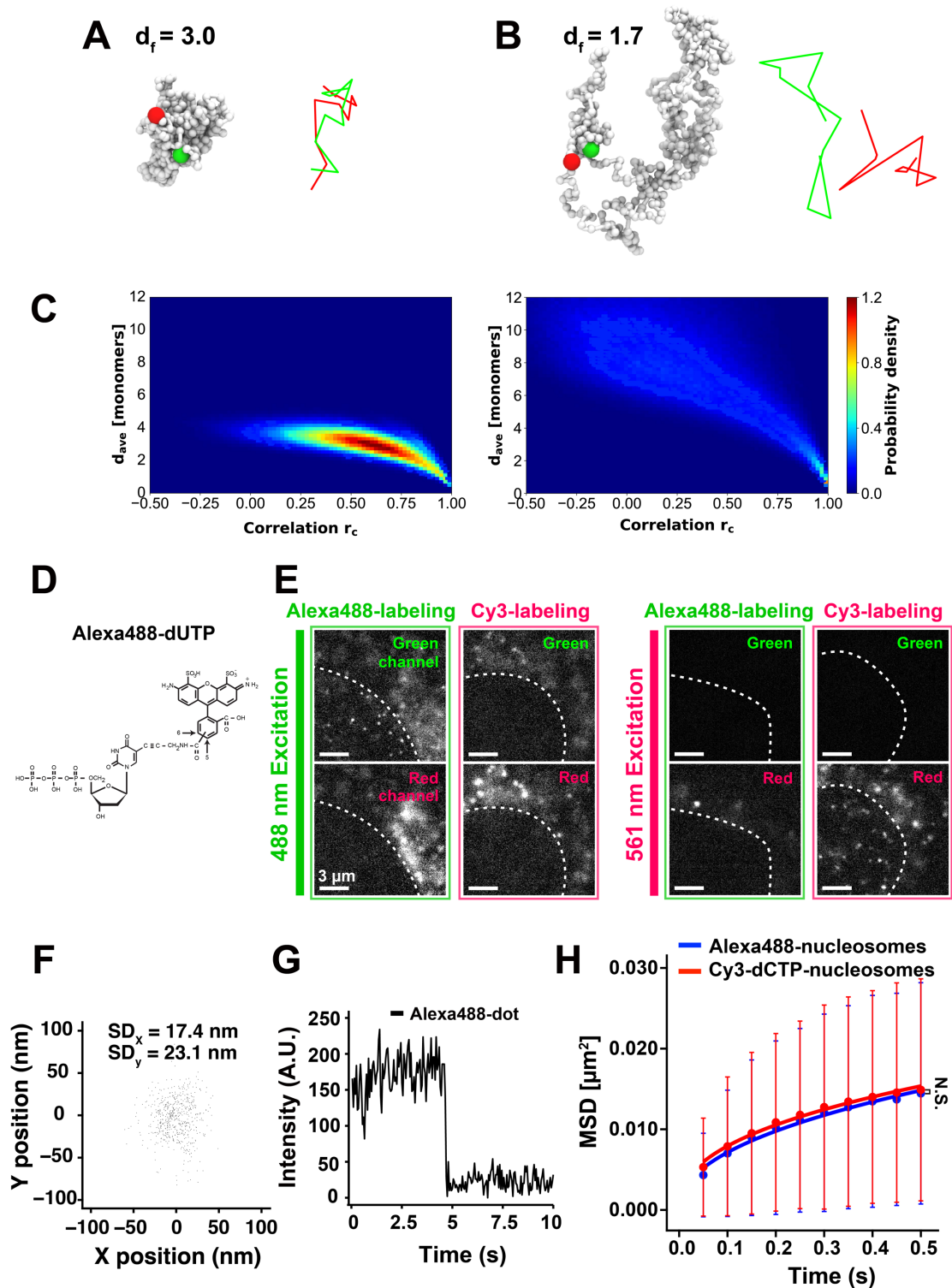


## Supplemental Figure S5

**Fig. S5. Single/dual-color single-nucleosome imaging in living human cells.**

(A) The position determination accuracy of Cy3-labeled nucleosomes. Distribution of nucleosome displacements from the initial localizations in the XY-plane in the 50-ms interval,  $n = 13$  nucleosomes in FA-fixed HeLa cells.  $SD_x$  and  $SD_y$  of fitted Gaussian functions were 13.9 nm and 15.3 nm, respectively. (B) Mean square displacement (MSD) plots of histone H2B-Halo-labeled nucleosomes without (blue) and with the electroporation

process (red) in living HeLa cells from 0 to 0.5 s. For each sample,  $n = 15$  cells. Not significant (N.S.;  $P = 0.93$ ) by Kolmogorov–Smirnov test. (C) Similar plots to (B), but from 0 to 3 s. Not significant (N.S.;  $P = 0.93$ ) by Kolmogorov–Smirnov test. (D) MSD plots of Cy3-labeled single-nucleosomes (red,  $n = 27$  cells) and H2B-Halo-labeled nucleosomes (blue, data were reproduced from (37)) in living HeLa cells from 0 to 0.5 s. The Kolmogorov–Smirnov test was used to determine P values. \*\*,  $P < 0.001$  for Cy3-labeled versus H2B-Halo-labeled nucleosomes ( $P = 3.1 \times 10^{-4}$ ). \*\*\*,  $P < 0.0001$  for Cy3-labeled versus FA-fixed Cy3-nucleosomes ( $P = 2.1 \times 10^{-13}$ ), H2B-Halo versus FA-fixed H2B-Halo nucleosomes ( $P = 5.7 \times 10^{-6}$ ). Not significant (N.S.) for FA-fixed Cy3-labeled versus FA-fixed H2B-Halo nucleosomes ( $P = 0.37$ ). (E) Log-log plots of MSD data shown in (D).

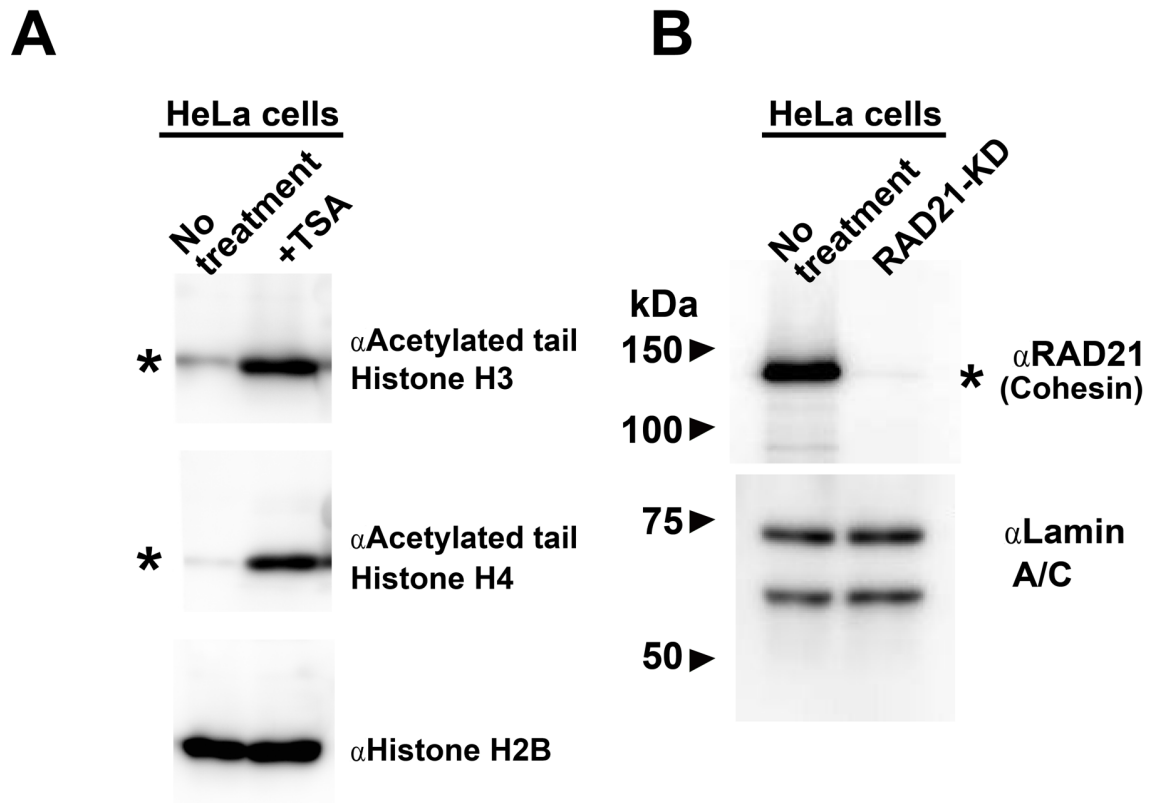


## Supplemental Figure S6

**Fig. S6. Dual-color single-nucleosome imaging in living human cells and computational modeling.**

(A, B) Simulation snapshots of Brownian dynamics for the fractal ring polymers with 500 nucleosomes, which mimics a condensed domain held by cohesin (A) and an extended fiber

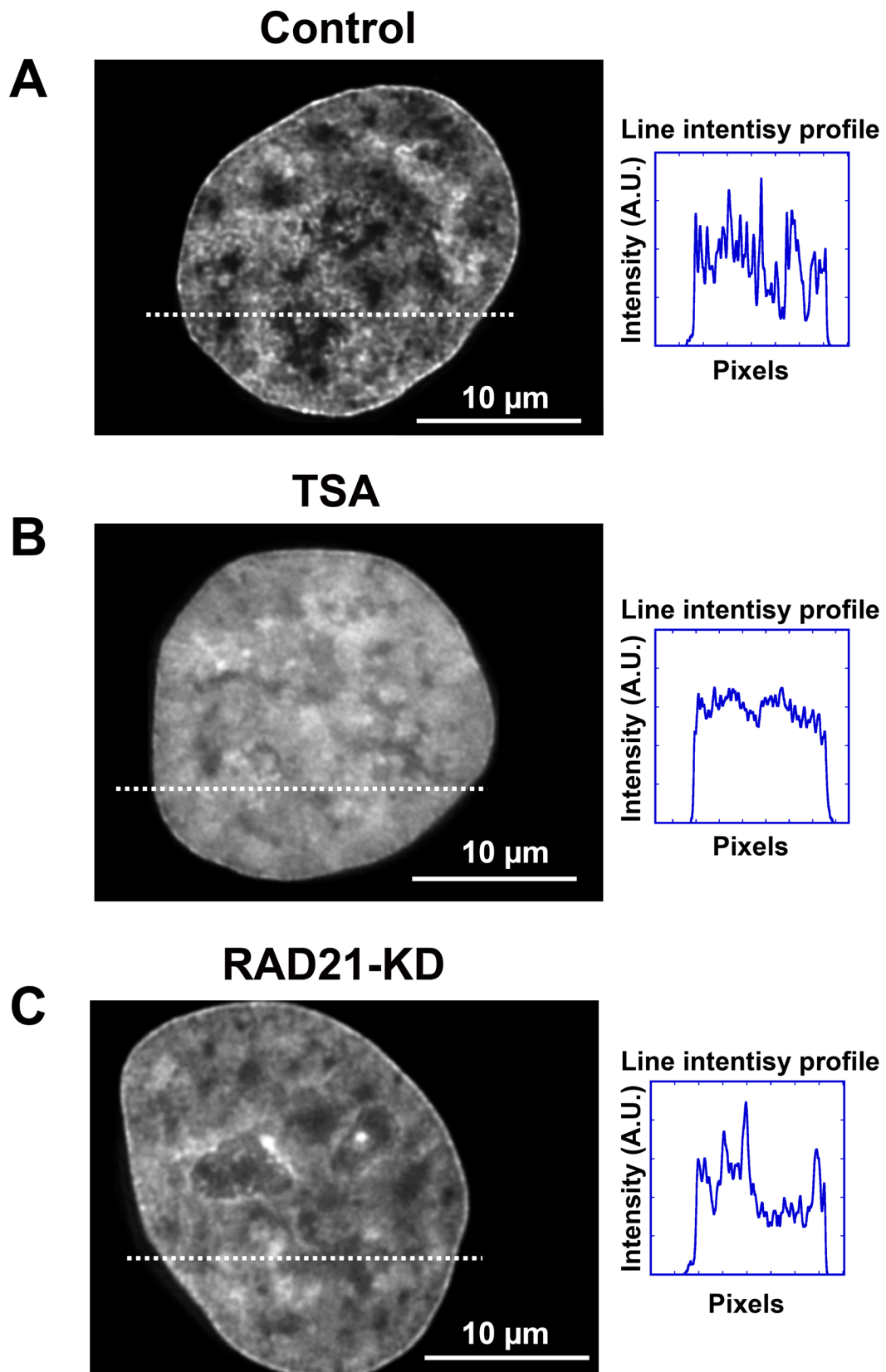
loop held by cohesin (B). Simulated trajectories (red and green) of the highlighted two nucleosomes on the XY-plane are shown on the right. (C) Distributions of the average distance in (A) and (B), normalized by the diameter of the monomer bead, between the two nucleosome beads versus their congruence coefficient  $r_c$  at the fractal dimension  $d_f = 3.0$  (left) and 1.7 (right) for 500 nucleosomes polymers. The heat map shows the probability density for a total of 1,000,000  $(r_c, d_{ave})$  pairs. Compared to the extended fiber loop structures (right,  $d_f = 1.7$ ), dynamics of condensed structures (left,  $d_f = 3.0$ ) cause positive and increased correlations in  $r_c$  between two randomly selected nucleosomes. (D) Structure of Alexa488-dUTP. (E) Fluorescent images for every combination of labeling/excitation /channel in a beam splitter system W-VIEW GEMINI. Note that there is essentially no crosstalk between the Alexa488 and Cy3 signals in our beam splitter system. (F) The position determination accuracy of Cy3-labeled nucleosomes through the beam splitter system. Distribution of nucleosome displacements from the initial localizations in the XY-plane in the 50-ms interval,  $n = 21$  nucleosomes in FA-fixed HeLa cells.  $SD_x$  and  $SD_y$  of fitted Gaussian functions were 17.4 nm and 23.1 nm, respectively. (G) Representative single-step photobleaching of Alexa488-labeled nucleosome (green in (E)). The vertical axis represents the fluorescence intensity and the horizontal axis is the tracking time series. A.U., arbitrary units. (H) MSD plots of single-nucleosomes labeled with Alexa488 (blue,  $n=14$  cells) and Cy3 (red,  $n=14$  cells) in living HeLa cells from 0 to 0.5 s. Note that deviations are much larger compared to those in Fig. S5D because the deviations of individual trajectories are shown.



## Supplemental Figure S7

**Fig. S7. Verifications of acetylated H3/H4 and cohesin depletion.**

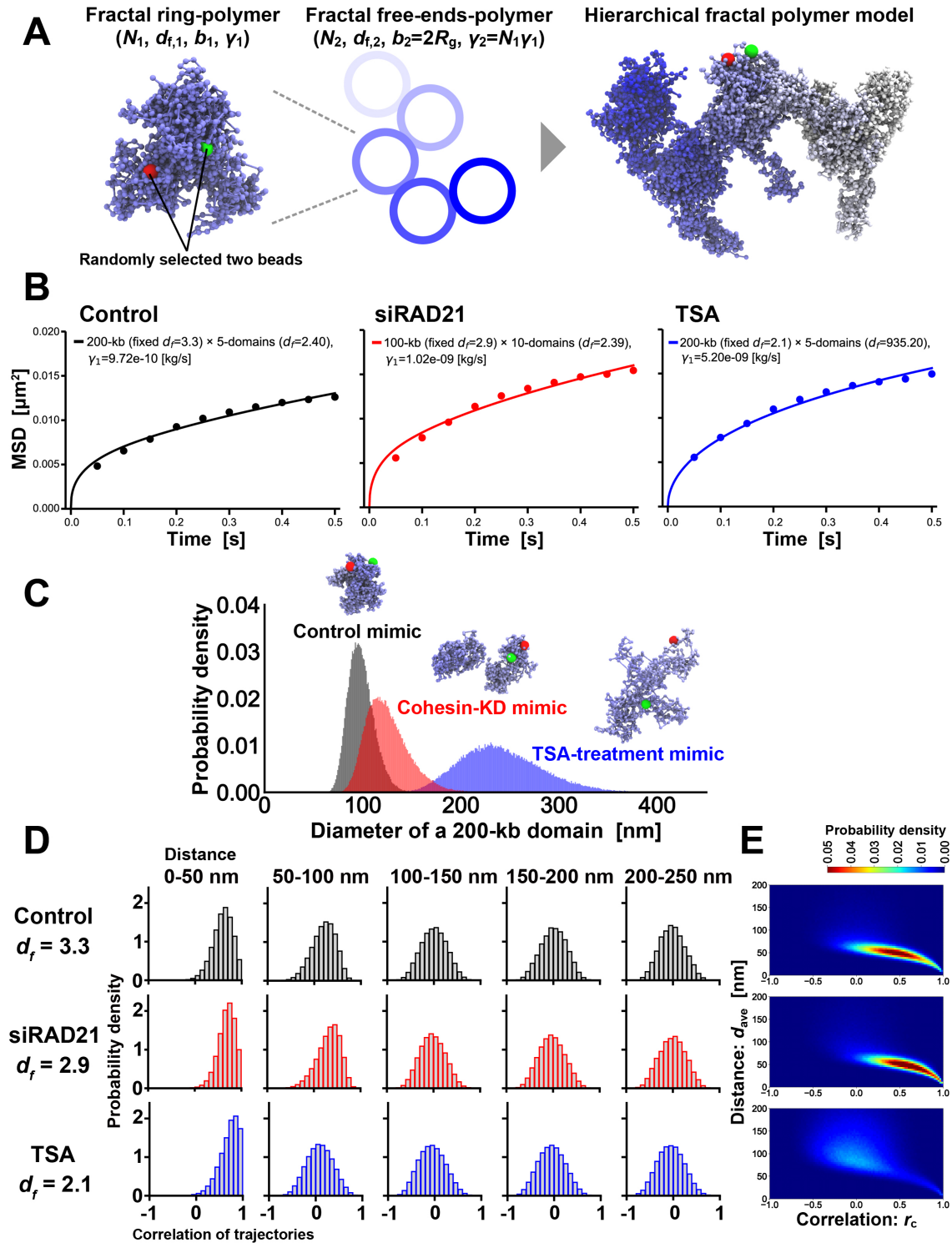
(A) Detection of histone H3 and H4 tail acetylation in HeLa cell lysates from untreated cells (left) and TSA-treated cells (right) by Western blotting with anti-acetylated H3 and H4 tail antibodies. Note the specific increase in histones H3 and H4 acetylation in the TSA-treated cells. Blotting result using anti-histone H2B antibody is shown as control. (B) Verification of RAD21 KD by Western blotting with anti-RAD21 antibody. For control, anti-lamin A/C antibody was used.



**Supplemental Figure S8**

**Fig. S8. Super-resolution images using STED (stimulated emission depletion) microscopy.**

Representative images of (A) untreated, (B) TSA-treated, and (C) RAD21-KD cells. These cells were fixed with formaldehyde and stained with SiR-Hoechst. Line intensity profiles corresponding to the dot lines on the images are shown on the right. A.U., arbitrary units.



## Supplemental Figure S9

**Fig. S9. Overview of the hierarchical fractal polymer model.**

(A) The hierarchical fractal polymer model comprises two layers. In the first layer,  $N_1$  nucleosome beads form a chromatin domain modeled by the ring-polymer with the fractal dimension  $d_{f,1}$ , the effective bond length between adjacent beads  $b_1$ , and the friction



coefficient of the beads  $\gamma_1$ . At the second layer,  $N_2$  chromatin domains sequentially connect, forming the free-ends-polymer with the fractal dimension  $d_{f,2}$ . The effective bond length  $b_2$  between adjacent domains corresponds to the diameter of gyration of the fractal ring-polymer  $b_2 = 2R_g$ , and the friction coefficient of the domains  $\gamma_2$  is  $N_1\gamma_1$ . **(B)** Fitting experimental MSD data (for control, siRAD21, and TSA) by our theoretical equation of the hierarchical fractal polymer model determines parameters  $\gamma_1$  and  $d_{f,2}$ , while parameters  $N_1$ ,  $N_2$ ,  $d_{f,1}$ , and  $T$  were fixed. **(C)** Distribution of diameter of 200-kb domains for control (black), cohesin-KD (siRAD21; red), and TSA-treatment (blue) models. **(D)** Probability densities of congruence coefficient  $r_c$  for control (top), siRAD21 (middle), and TSA (bottom) models calculated between the two nucleosome beads whose average distances were in the ranges of 0–50 nm, 50–100 nm, 100–150 nm, 150–200 nm, and 200–250 nm in 500 ms. **(E)** Heatmaps of the two-dimensional probability density of 1,000,000 pairs of the congruence coefficient  $r_c$  and the average distance  $d_{ave}$ . The sorting order corresponds to (D).

**Table S1. ChIP-seq data of histone marks.**

<b>ID *</b>	<b>Histone target</b>	<b>Function</b>	<b>Overlap with Cy3-labeled regions (%)</b>	<b>URL</b>
ENCFF108DAJ	H3K4me2	TA	62.73	<a href="https://www.encodeproject.org/experiments/ENCSR000AOE/">https://www.encodeproject.org/experiments/ENCSR000AOE/</a>
ENCFF447CLK	H3K4me3	TA	65.70	<a href="https://www.encodeproject.org/experiments/ENCSR000AOF/">https://www.encodeproject.org/experiments/ENCSR000AOF/</a>
ENCFF723WDR	H3K9ac	TA	68.55	<a href="https://www.encodeproject.org/experiments/ENCSR000AOH/">https://www.encodeproject.org/experiments/ENCSR000AOH/</a>
ENCFF144EOJ	H3K27ac	TA	65.74	<a href="https://www.encodeproject.org/experiments/ENCSR000AOC/">https://www.encodeproject.org/experiments/ENCSR000AOC/</a>
ENCFF916VLX	H3K79me2	TA	62.10	<a href="https://www.encodeproject.org/experiments/ENCSR000AOG/">https://www.encodeproject.org/experiments/ENCSR000AOG/</a>
ENCFF001SVY	H3K36me3	TA	75.80	<a href="https://www.encodeproject.org/experiments/ENCSR000AOD/">https://www.encodeproject.org/experiments/ENCSR000AOD/</a>
ENCFF162RSB	H3K4me1	TA	63.05	<a href="https://www.encodeproject.org/experiments/ENCSR000APW/">https://www.encodeproject.org/experiments/ENCSR000APW/</a>
ENCFF252BLX	H3K27me3	TS	14.62	<a href="https://www.encodeproject.org/experiments/ENCSR000APB/">https://www.encodeproject.org/experiments/ENCSR000APB/</a>

**Abbreviations: TA, transcriptional activation; TS, transcriptional silencing.**

**\* FileTypes were derived from replicated peaks.**

**Movie S1.**

Video of Cy3-labeled single-nucleosomes in a HeLa nucleus. The single-nucleosomes were recorded at 50 ms/frame, and the pixel size is 65 nm in this video. Note that, after background subtraction, clear, well-separated dots and their movements were visualized with a single-step photobleaching profile (see Fig. 2E), suggesting that each dot represents a single-nucleosome labeled by single Cy3.

**Movie S2.**

The tracked data by u-track (MATLAB package; (59)) was overlaid on the original movie and marked with red circles (right). Dots tracked more than 3 frames were analyzed.

**Movie S3.**

A Brownian dynamics simulation of a condensed chromatin structure modeled by a fractal ring-polymer with 500 nucleosome beads and fractal dimension  $d_f = 3.0$ . The highlighted green and red spheres represent two randomly labeled single-nucleosome beads.

**Movie S4.**

A Brownian dynamics simulation of an extended-loop chromatin structure modeled by a fractal ring-polymer with 500 nucleosome beads and fractal dimension  $d_f = 1.7$ . The highlighted green and red spheres represent two randomly labeled single-nucleosome beads.

**Movie S5.**

Video of two close labeled single-nucleosomes (left, labeled by Alexa488; right, Cy3). The two single-nucleosomes were recorded simultaneously at 50 ms/frame using W-VIEW GEMINI (Hamamatsu Photonics), and the pixel size is 65 nm in this video. Note that these two nucleosomes show correlative motion.

**Movie S6.**

Another example of S5.

**Movie S7.**

Video of two distant labeled single-nucleosomes (left, labeled by Alexa488; right, Cy3). The two single-nucleosomes were recorded simultaneously at 50 ms/frame using W-VIEW

GEMINI (Hamamatsu Photonics) and put together side by side. The pixel size is 65 nm in this video. Note that movements of two nucleosomes are not correlated.

**Movie S8.**

Another example of S7.

**Movie S9.**

A Brownian dynamics simulation of five domains that mimics the untreated control. The domain is modeled by a fractal ring-polymer with 1000 beads and the fractal dimension  $d_f = 3.3$ . The highlighted green and red spheres represent two randomly labeled single-nucleosome beads. The frame rate is 5  $\mu\text{s}/\text{frame}$ .

**Movie S10.**

A 200-kb-sized single domain is highlighted from Movie S9.

**Movie S11.**

A Brownian dynamics simulation of five domains that mimics the TSA-treated (i.e., rather extended) domains. The domains were modeled by a fractal ring-polymer with 1000 beads and the fractal dimension  $d_f = 2.1$ . The highlighted green and red spheres represent two randomly labeled single-nucleosome beads. The frame rate is 5  $\mu\text{s}/\text{frame}$ .

**Movie S12.**

A 200-kb-sized single domain is highlighted from Movie S11.

**Movie S13.**

A Brownian dynamics simulation of ten half-sized domains that mimics the cohesin-KD chromatin. The domains were modeled by a fractal ring-polymer with 500 beads and the fractal dimension  $d_f = 2.9$ . The highlighted green and red spheres represent two randomly labeled single-nucleosome beads. The frame rate is 5  $\mu\text{s}/\text{frame}$ .

**Movie S14.**

Two 100-kb-sized domains are highlighted from Movie S13.

**Movie S15.**

Video of early replication foci labeled with Cy3 in a HeLa nucleus. Replication foci were recorded at 50 ms/frame, and the pixel size is 65 nm in this video.

**Movie S16.**

Representative video of fluorescent recovery after photobleaching (FRAP) of Cy3-labeled early replication foci in a HeLa nucleus. For time-lapse imaging, 60 frames were acquired at 30 seconds per frame. XY-movement of the cell is corrected.